The circadian PAR-domain basic leucine zipper transcription factors DBP, TEF, and HLF modulate basal and inducible xenobiotic detoxification

Frédéric Gachon,[1,3] Fabienne Fleury Olela,[1] Olivier Schaad,[2] Patrick Descombes,[2] and Ueli Schibler[1,*]

[1] Department of Molecular Biology, National Center of Competence in Research "Frontiers in Genetics," Sciences III, University of Geneva, 1211 Geneva 4, Switzerland
[2] Genomics Platform, National Center of Competence in Research "Frontiers in Genetics," Medical Center of the University of Geneva, Rue Michel-Servet 1, CH-1206 Geneva, Switzerland
[3] Present address: Institut de Génétique Humaine, CNRS UPR 1142 , 141, rue de la Cardonille 34396, Montpellier Cedex 5, France.
*Correspondence: ueli.schibler@molbio.unige.ch

Summary

The PAR-domain basic leucine zipper (PAR bZip) transcription factors DBP, TEF, and HLF accumulate in a highly circadian manner in several peripheral tissues, including liver and kidney. Mice devoid of all three of these proteins are born at expected Mendelian ratios, but are epilepsy prone, age at an accelerated rate, and die prematurely. In the hope of identifying PAR bZip target genes whose altered expression might contribute to the high morbidity and mortality of PAR bZip triple knockout mice, we compared the liver and kidney transcriptomes of these animals to those of wild-type or heterozygous mutant mice. These experiments revealed that PAR bZip proteins control the expression of many enzymes and regulators involved in detoxification and drug metabolism, such as cytochrome P450 enzymes, carboxylesterases, and constitutive androstane receptor (CAR). Indeed, PAR bZip triple knockout mice are hypersensitive to xenobiotic compounds, and the deficiency in detoxification may contribute to their early aging.

Introduction

The circadian mammalian timing system has a hierarchical structure, in that a master pacemaker in the suprachiasmatic nucleus (SCN) of the brain's hypothalamus synchronizes self-sustained and cell-autonomous circadian oscillators present in virtually all tissues. Interconnected feedback loops in clock gene expression are believed to be the centerpieces of the molecular clockwork circuitry in both SCN neurons and peripheral cells (Reppert and Weaver, 2002). In mammals, the circadian timing system controls many aspects of behavior and physiology, including rest-activity cycles, heartbeat frequency, body temperature, arterial blood pressure, endocrine functions, renal plasma flow, intestinal peristalsis, and metabolism (Gachon et al., 2004b).

The circadian oscillators in peripheral cells can mediate rhythmic physiology through circadian transcription factors, which in turn regulate the transcription of downstream genes. The three PAR-domain basic leucine zipper (PAR bZip) proteins DBP, TEF, and HLF are examples of such output mediators, since they are transcriptionally regulated by core oscillator components (Ripperger and Schibler, 2006; Ripperger et al., 2000; B. Kornmann and U.S., unpublished data), but have little effect on circadian behavior and clock genes expression (Gachon et al., 2004a). These proteins activate transcription of downstream genes by binding as homo- or heterodimers to DNA elements matching the consensus sequence RTTAYGTAAY or slight variations thereof (Falvey et al., 1996). While DBP and TEF accumulate in most peripheral cell types, the expression of HLF is restricted to a subset of tissues, including liver and kidney (Falvey et al., 1995; Fonjallaz et al., 1996).

Mice deficient of only one or two PAR bZip genes display relatively mild phenotypes (Franken et al., 2000; Gachon et al., 2004a; Lopez-Molina et al., 1997), in spite of the extraordinarily high amino acid sequence conservation of each of the three family members during mammalian evolution (see Figure S1). However, strong phenotypes are observed when all three PAR bZip genes are inactivated. Thus, about half of these animals succumb to spontaneous and sound-induced epileptic seizures during the first 3 months after birth (Gachon et al., 2004a). Individuals surviving this time span rarely die of epileptic attacks but after nine months of age exhibit signs diagnostic for early aging, such as cachexia, lordokyphosis, and an absence of vigor. All in all, less than 20% of PAR bZip triple knockout animals reach an age of 1 year (Gachon et al., 2004a; F.G. and U.S., unpublished data).

Since it is unlikely that the epileptic seizures account for all of the phenotypes described above, we suspected that the loss of PAR bZip proteins in tissues other than brain contributes to precocious aging and premature death. We thus initiated a study aimed at the elucidation of putative functions of PAR bZip proteins in liver and kidney, two organs in which all three family members are expressed. Our experiments revealed that in both tissues, DBP, TEF, and HLF regulate the expression of numerous genes involved in the metabolism of endobiotic and xenobiotic substances, and that PAR bZip triple knockout mice display an impaired defense against xenobiotic stress.

Results

PAR bZip proteins control the expression of genes involved in xenobiotic detoxification

To identify putative PAR bZip target genes, we compared mRNA expression profiles in liver of PAR bZip proficient ($H^{+/+}/D^{+/+}/T^{+/+}$ or $H^{+/-}/D^{+/-}/T^{+/-}$) and deficient ($H^{-/-}/D^{-/-}/T^{-/-}$) mice. All animals were sacrificed at ZT12 (ZT = *Zeitgeber* time; ZT00: lights on, ZT12: lights off), when the PAR bZip target genes were expected to approach maximum expression levels (see Figure S4). Three pools of liver or kidney RNA, composed of equivalent amounts of RNA from three males and three females each, were compared by hybridization to Affymetrix oligonucleotide microarrays representing virtually all protein-encoding mouse genes. As PAR bZip proteins are transcriptional activators, we expected transcripts specified by direct target genes to be less abundant in the triple knockout mice as compared to wild-type or triple heterozygous animals. Figures 1A and 1B display the results of pairwise comparisons between liver RNAs from triple knockout and wild-type mice (panel A) and triple knockout and triple heterozygous animals (panel B). The Venn diagram depicted in Figure 1D illustrates that approximately 62% of the differentially expressed genes found in the comparison of triple knockout with triple heterozygous mice were also found in the comparison of triple knockout with wild-type mice. We also used homo- and heterozygous triple knockout mice for the comparison of kidney transcriptomes (Figure 1C) since these mice are genetically more closely related than homozygous knockout and wild-type mice and since the comparison of heterozygous with homozygous knockout mice displayed less noise for differentially expressed genes than that of wild-type mice with homozygous knockout mice (Figure S3). As illustrated by the Venn diagram in Figure 1E, 14 of the 77 transcripts downregulated in the kidney of $H^{-/-}/D^{-/-}/T^{-/-}$ mice were also detected at lower concentrations in the liver of $H^{-/-}/D^{-/-}/T^{-/-}$ mice. Many of the genes differentially expressed in liver and/or kidney of $H^{-/-}/D^{-/-}/T^{-/-}$ mice are involved in the metabolism of lipids or xenobiotic substances, and some of them, e.g., those encoding carboxylesterase (Satoh and Hosokawa, 1998) and members of the cytochrome P450 family (*Cyp4a* and *Cyp2c*), are implicated in both of these pathways (Anzenbacher and Anzenbacherova, 2001; Wang et al., 2004). Constitutive androstane receptor (*CAR*) appeared to be a particularly interesting PAR bZip target gene in liver (see Tables S1 and S2), although the difference revealed by Affymetrix hybridization experiments was below the arbitrarily set threshold value of 1.8 applied in Figure 1. The nuclear receptor (NR1I3) specified by this gene is an important sensor of xenobiotic substances and mediates the drug-induced transcription of various detoxification enzymes (Handschin and Meyer, 2005; Qatanani and Moore, 2005). Pleasingly, the microarray experiments indicated that known CAR target genes, such as members of the *Cyp2b* and *Cyp3a* families (Maglich et al., 2002, 2004; Staudinger et al., 2003; Ueda et al., 2002), were also downregulated in $H^{-/-}/D^{-/-}/T^{-/-}$ mice (Figure 1). Additional PAR bZip target genes related to the detoxification of xenobiotics or the scavenging of reactive oxygen species (ROS) encode members of the sulfotransferase family (*Sult1d1*, *Sult3a1*), the glutathion-S-transferase family (*GSTt1*, *Gsta2*, *Gsta3*), the aldehyde dehydrogenase family (*Aldh1a1*, *Aldh1a7*, *Aldh3a2*), the UDP-glucuronosyltransferase family (*Ugt1a1*, *Ugt2b37*), and the drug transporter family (*AbcG2*, *AbcC4*, *AbcA8a*, *AbcA6*, *AbcB1b*). Interestingly, all of these gene families are also known targets of the CAR pathway. Aminolevulinic acid synthase (ALAS1) and P450 oxidoreductase (POR) are two CAR-regulated enzymes with a particularly wide spectrum in xenobiotic detoxification. ALAS1 is the rate-limiting enzyme in the synthesis of heme, the prosthetic group of all cytochrome P450 enzymes, and POR provides the electrons required for all cytochrome P450-mediated monooygenase reactions (Gutierrez et al., 2003). Additional target genes of PAR bZip factors are *Rad51l1* and *Dclre1a*, involved in DNA repair, *Biklk* controlling apoptosis, *Wee1*, a major regulator of mitosis, and *Per3*, a period isoform with unknown functions (for a complete list of the differentially expressed genes, see Tables S1, S2, and S3).

We also found transcripts that are more abundant in homozygous triple knockout animals as compared to wild-type or heterozygous triple knockout animals (Figures S2). We suspect that the synthesis of these mRNAs is indirectly influenced by PAR bZip transcription factors, for example by repressors whose expression is controlled by PAR bZip proteins or as a consequence of liver damage in PAR bZip-deficient mice (see below). We could not recognize an obvious functional pattern in the set of upregulated genes but noticed that their expression shows a greater variability than those that are downregulated in PAR bZip knockout mice, at least in the genetically matched homozygous and heterozygous littermates (see Figure S3).

Temporal transcription of PAR bZip target genes

Given the circadian accumulation of DBP, TEF, and HLF in liver and kidney, we expected that the direct target genes of these transcription factors would also be transcribed in a cyclic manner. Based on a simple mathematical simulation of circadian mRNA accumulation (Figure S4), we anticipated a wide range of amplitudes but a relatively narrow range of phases with peaks between ZT12 and ZT16 for the expression of direct PAR bZip target genes. Figure 2 depicts Northern blot and ribonuclease protection experiments showing the temporal accumulation profiles for some of these transcripts in liver (panel A) and kidney (panel B). As expected, the accumulation of these mRNAs showed large differences in amplitudes and in the degree to which it depended on PAR bZip proteins. For example, in kidney carboxylesterase 3 (*Ces3*), mRNA levels clearly oscillated during the day and were nearly undetectable in homozygous triple knockout mice. The observed circadian change in the size of the transcript is probably due to a shortening of the poly(A) tail in aging mRNA molecules. *CAR*, and *AK3l1* transcripts in liver, and *Cyp2a5* transcript in kidney also fluctuated in abundance but were still produced at basal levels in PAR bZip triple knockout mice. While *RGS16* mRNA accumulates in a strongly diurnal fashion, the phase is not compatible with that expected for a transcript encoded by a direct PAR bZip target gene. The *Alas1* mRNA accumulation profiles in wild-type and heterozygous animals would be compatible with a direct PAR bZip regulatory mechanism. However, these transcripts were still expressed at high levels in PAR bZip-deficient mice, albeit with a dramatically different phase. Hence PAR bZip protein-independent control mechanisms must have contributed to the rhythmic *Alas1* transcription in triple knockout mice. In kidney, circadian *Bhmt* mRNA accumulation was clearly controlled by PAR bZip proteins. Yet, the phase of this cycle suggested an

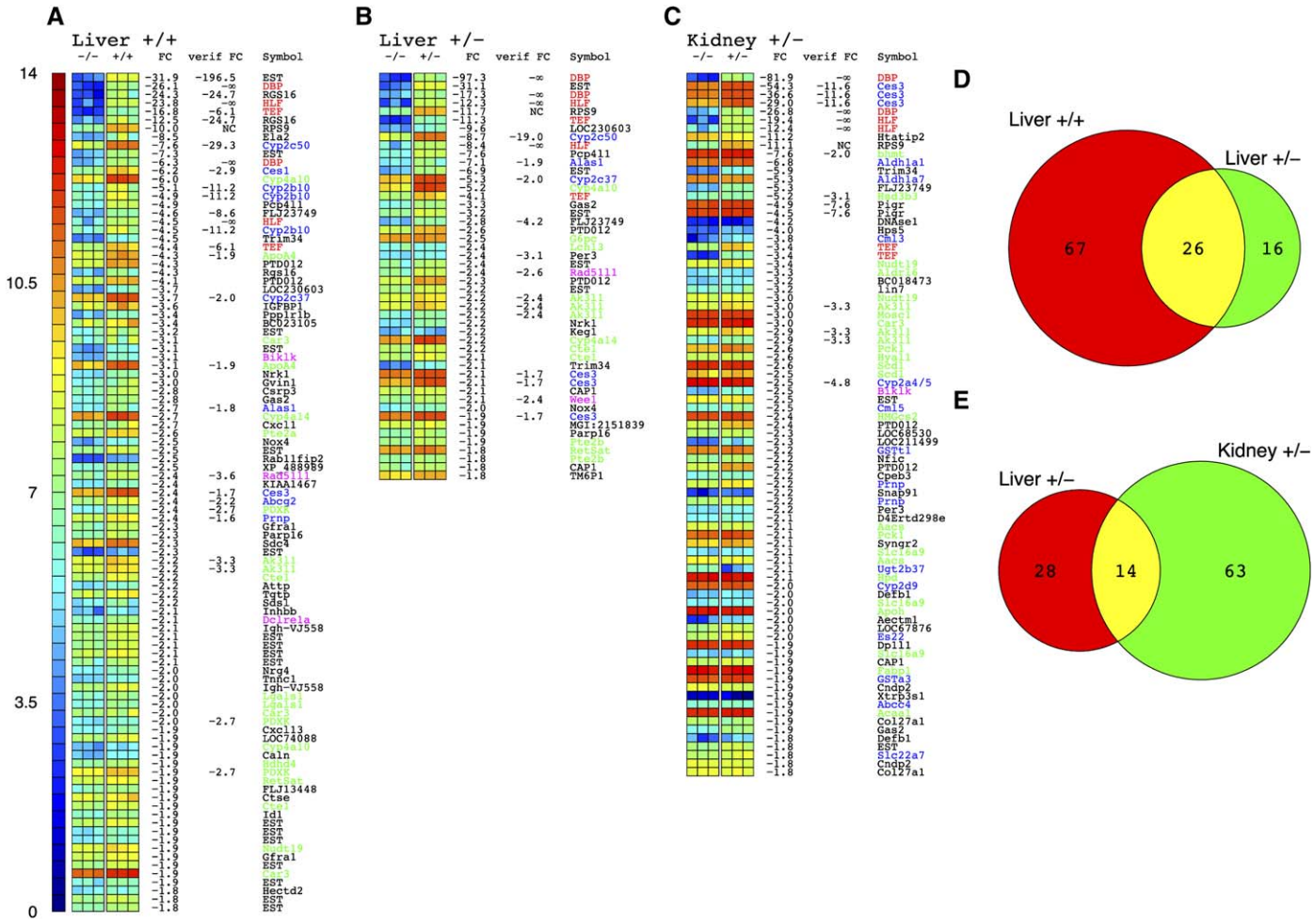

Figure 1. Identification of putative PAR bZip target genes by Affymetrix microarray analysis

Transcripts whose abundance was at least 1.8-fold higher in PAR bZip -(+/+ or +/−) as compared to PAR bZip-deficient (−/−) mice are listed in (**A**) to (**C**).
A) Liver transcripts that are less abundant in homozygous triple knockout mice ($H^{-/-}/D^{-/-}/T^{-/-}$) as compared to wild-type mice ($H^{+/+}/D^{+/+}/T^{+/+}$).
B) Liver transcripts that are less abundant in homozygous triple knockout mice ($H^{-/-}/D^{-/-}/T^{-/-}$) as compared to heterozygous triple knockout mice ($H^{+/-}/D^{+/-}/T^{+/-}$).
C) Kidney transcripts that are less abundant in homozygous triple knockout mice ($H^{-/-}/D^{-/-}/T^{-/-}$) as compared to heterozygous triple knockout mice ($H^{+/-}/D^{+/-}/T^{+/-}$).
The color scale to the left of the panels represents expression levels of each transcript in the three RNA pools used for each analysis. The fold change is the average value of all nine comparisons. The verified fold change indicates the relative accumulation values as estimated by Northern blot or ribonuclease protection experiments. Colored letters indicate the putative functions of genes: red: PAR bZip, bBlue: detoxification, green: metabolism, magenta: apoptosis, cell-cycle control, and DNA repair.
D) Venn diagrams comparing the differentially expressed liver transcripts shown in (**A**) and (**B**). The shared 26 transcripts (yellow) are downregulated in both comparisons.
E) Venn diagrams comparing the differentially expressed liver and kidney transcripts shown in (**B**) and (**C**). The shared 14 transcripts (yellow) are downregulated in both comparisons.

indirect regulatory mechanism. *Cyp2c50* mRNA accumulation also depended strongly on PAR bZip proteins, but it was nearly constant throughout the day in wild-type and heterozygous knockout mice. Interestingly, however, the levels of *Cyp2c50* pre-mRNA still oscillated with about 3-fold amplitude (Figure 2C), suggesting that the temporally invariable *Cyp2c50* mRNA accumulation was probably caused by a long half-life (see Figure S4D). The expression of some of these genes in the liver was also quantified by qRT-PCR. These results confirmed the Northern blot data with respect to circadian expression and differences between wild-type and triple knockout animals at ZT12 (Figure S5).

Direct PAR bZip target genes are expected to harbor PARREs (*PAR* bZip-*R*esponsive *E*lements) in the vicinity of their transcription initiation sites. Indeed, sequences with strong homologies to PARREs could be identified in several of these genes (Figure 3). The ability of the PARREs associated with the promoters of *Ces3* (a gene involved in detoxification and drug metabolism, see Satoh and Hosokawa, 1998) and *AK3l1* (Figures 3A and 3B) to bind PAR bZip transcription factors in vitro was verified by electrophoretic mobility shift assays (EMSA) (Figure 3C). While the results obtained in these experiments are in keeping with the direct transactivation of *Ces3* and *AK3l1* transcription by Par bZip proteins, they can obviously not exclude indirect mechanisms.

The data presented in Figure S6 suggest that DBP, TEF, and HLF carry out partially redundant functions. Thus, *AK3l1* and *CAR* mRNAs accumulated to near wild-type levels in all single and double mutant mice. *Ces3*, *Cyp2c50*, or *Cyp2a4* did show a somewhat reduced expression in *Hlf-Tef* double knockout

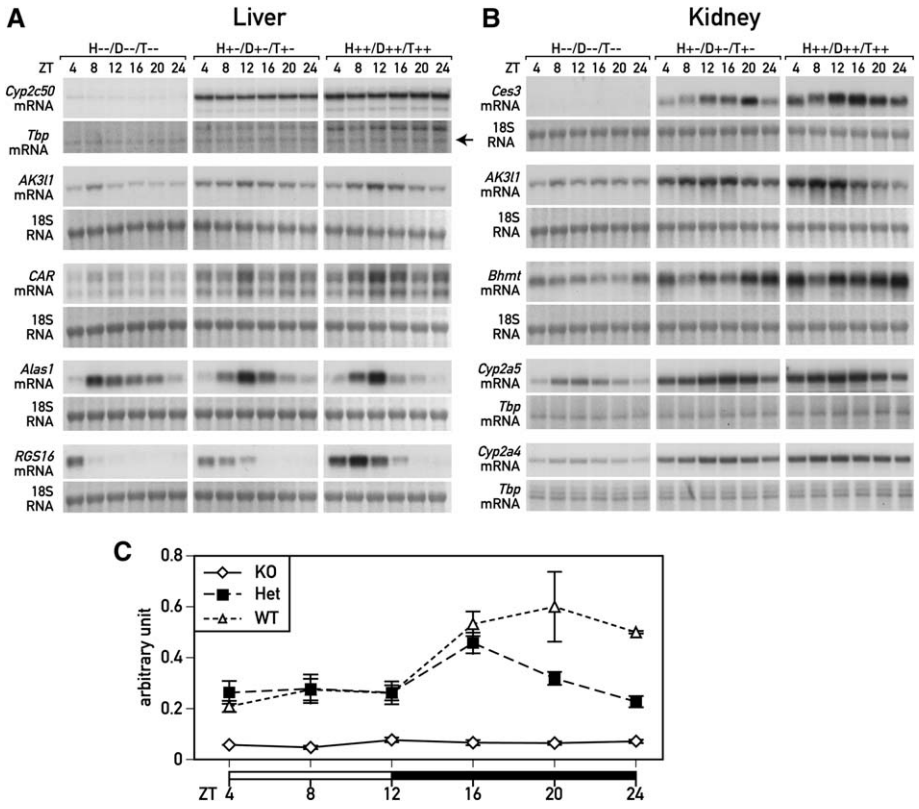

Figure 2. Temporal expression of transcripts specified by putative PAR bZip target genes

A and B) Northern blot (*AK3l1*, *CAR*, *Alas1*, *RGS16*, *Ces3*, *Bhmt*) and ribonuclease protection (*Cyp2c50*, *Cyp2a5*, and *Cyp2a4*) experiments were conducted with whole-cell RNAs of livers and kidneys of homozygous triple knockout ($H^{-/-}/D^{-/-}/T^{-/-}$), heterozygous triple knockout, ($H^{+-}/D^{+-}/T^{+-}$), and wild-type ($H^{++}/D^{++}/T^{++}$) mice. For Northern blot experiments, the membranes were stained with methylene blue before hybridization and stained 18S rRNA is shown as a loading reference. For ribonuclease protection assays, a *Tbp* probe was used as a control (Schmidt and Schibler, 1995). The *Zeitgeber* times (ZT) at which the animals were sacrificed are indicated on the top of the figure.

A) Temporal expression of putative PAR bZip target genes in liver.

B) Temporal expression of putative PAR bZip target genes in kidney.

C) Temporal expression of *Cyp2c50* pre-mRNA in liver, as monitored by Taqman real-time RT-PCR with an amplicon located within intron 7. The data are normalized to the values obtained by the same procedure for an amplicon within *Tbp* mRNA. Mean values ± SEM obtained from three independant samples are given in the diagram.

mice, but these expression levels were still higher than those observed in triple knockout mice. As judged on the basis of the results obtained with double knockout mice, TEF and HLF alone activate these three genes more efficiently than DBP alone. Nevertheless, all three PAR bZip proteins did show some functional redundancy for all examined target genes.

CAR-dependent induction of *Cyp2b10* transcription is blunted in PAR bZip triple knockout mice

CAR is expressed in hepatocytes and epithelium villi cells of the small intestine (Handschin and Meyer, 2005; Qatanani and Moore, 2005). Similar to steroid hormone receptors, CAR is sequestered in inert complexes with chaperones and cochaperones in the absence of activating substances. Upon activation with xenobiotic compounds, such as barbiturates, CAR dissociates from these complexes and stimulates target gene transcription as a heterodimer with retinoid-X receptor (RXR) (Ueda et al., 2002; Swales and Negishi, 2004). As shown in Figure 2A, *CAR* mRNA accumulation in liver was circadian (2.5-fold amplitude) in wild-type mice but constitutively low in PAR bZip-deficient mice (3-fold downregulation at ZT12). In keeping with this finding, the CAR target gene *Cyp2b10* was expressed at very low levels throughout the day in $H^{-/-}/D^{-/-}/T^{-/-}$ mice. However, significant amounts of mRNA could be detected between ZT16 and ZT24 in $H^{+/+}/D^{+/+}/T^{+/+}$ and $H^{+/-}/D^{+/-}/T^{+/-}$ animals (Figure 4A), when CAR expression is high and when the animals feed. The somewhat erratic levels of *Cyp2b10* transcripts during these daytimes reflected interindividual variability (see Figure S7). Conceivably, the time and extent of CAR-dependent detoxification of food constituents depend on individual feeding habits.

Next, we analyzed *Cyp2b10* mRNA levels in liver and small intestine before and 4 hr after intraperitoneal injection of phenobarbital at different daytimes to investigate whether the daytime-dependent induction of *Cyp2b10* transcription differed between PAR bZip-proficient and -deficient mice (Figure 4B). Small intestine and liver are both important organs involved in xenobiotic detoxification. In both of these organs, *CAR* mRNA is rhythmically expressed and downregulated in triple knockout mice. Moreover, the activity of small intestine is probably also daytime dependent, as judged by the circadian clock gene expression observed in this organ (Figure S8). In both liver and small intestine, phenobarbital injections efficiently induced *Cyp2b10* mRNA expression (e.g., 400-fold in the liver at ZT16). In all cases, drug-induced accumulation of *Cyp2b10* mRNA was strongly attenuated in triple PAR bZip knockout mice (approximately 7-fold in both organs) and oscillated with a 2.5-fold and 8-fold amplitude in liver and small intestine, respectively, of wild-type mice (Figure 4C).

EMSA experiments with a high affinity CAR binding site (*Cyp2b10* NR1, see Honkakoski et al., 1998) and nuclear extracts from liver and small intestine corroborated the positive role of CAR in drug-induced *Cyp2b10* RNA expression (Figure 4D, left top panel). Thus, in the liver of wild-type animals, NR1 binding activities increased strongly after phenobarbital injection, and this increase was higher at ZT16 than at ZT4. In contrast, phenobarbital treatment elicited only a moderate enhancement of NR1 binding activity in PAR bZip triple knockout animals, and the observed induced levels were similarly low at both times of injection.

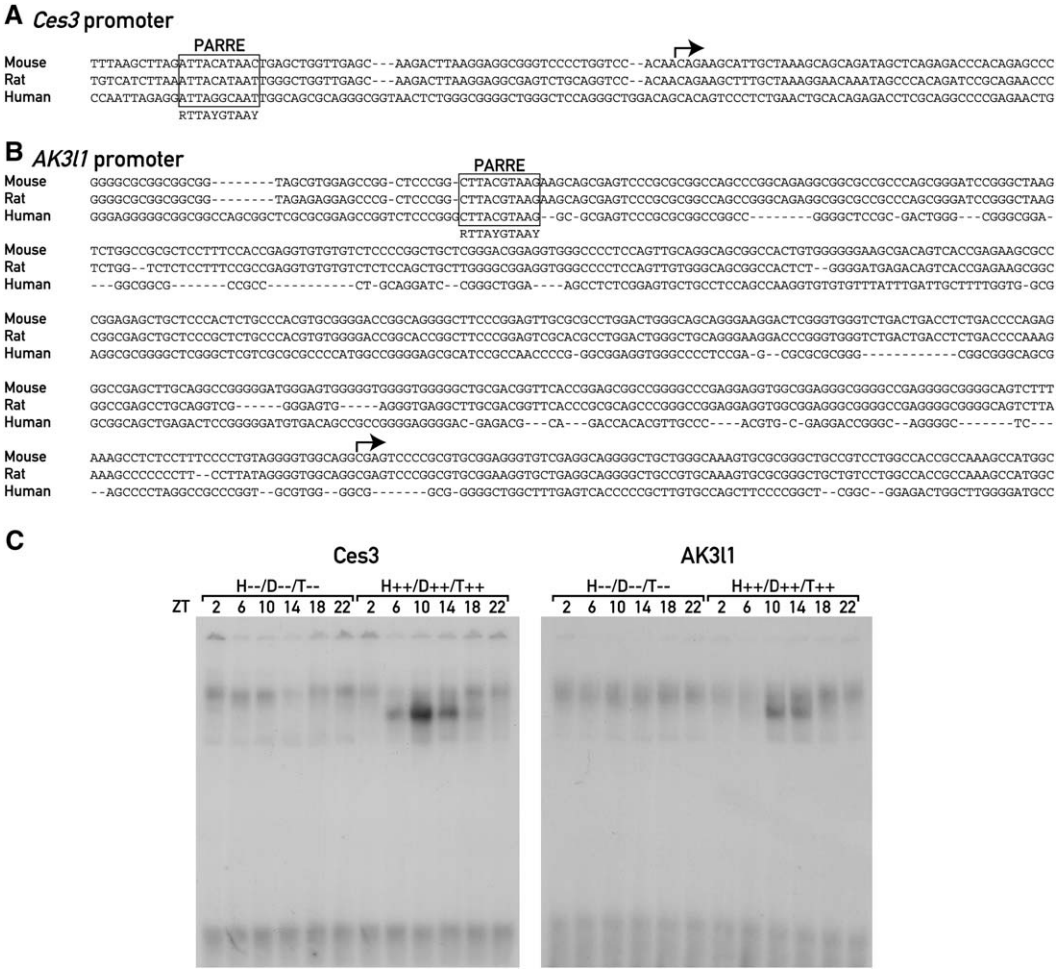

Figure 3. In vitro binding of PAR bZip proteins to PARRE elements within the *Ces3* and *AK3l1* promoters

A and B) Sequence comparisons of the 5′-flanking region of the *Ces3* and *AK3l1* genes from mouse, rat, and man. The transcription initiation sites are indicated by arrows. PAR bZip transcription factor Response Elements (PARRE) are located in the vicinity of the transcription start site. The PARRE consensus sequence is given below the element (R = A or G, Y = C or T).

C) In vitro binding of liver nuclear proteins to PARREs. Electrophoretic mobility shift assays (EMSA) were carried out with a radiolabeled oligonucleotide encompassing the PARREs of *Ces3* and *AK3l1*, respectively, and liver nuclear proteins from triple knockout mice and wild-type animals were harvested at 4 hr intervals around the clock.

In the experiments with small intestine nuclear extracts, we had to resort to a two-dimensional EMSA technique (Ossipow et al., 1993) to visualize phenobarbital-induced protein-DNA complexes, presumably because the low levels of CAR-DNA complexes in this tissue were masked by other NR1 binding activities (Figure 4D, right top panel). This more refined analysis revealed several phenobarbital-induced NR1 binding proteins in both liver and small intestine (Figure 4D, lower panels), and at least some of these corresponded to CAR isoforms (see Figure S9). As expected, these phenobarbital-induced proteins were more abundant at ZT16 than at ZT4 in both examined tissues.

PAR bZip proteins influence the expression of enzymes involved in all cytochrome P450-mediated monooxygenase reactions

Cytochrome P450 monooxygenases are membrane bound heme-enzymes that use molecular oxygen to hydroxylate endobiotic and xenobiotic substances. Depending on the compound, this hydroxylation could activate or inactivate the substrate. P450 oxidoreductase (POR), a flavin- and flavin-mononucleotide-containing electron transporter, transfers the electrons required for this reaction from NADPH to the heme bound iron-oxygen complex of cytochrome P450 enzymes (Gutierrez et al., 2003). The expression of functional cytochrome P450 enzymes must therefore be coordinated with that of POR, the electron provider, and ALAS1, the rate-limiting enzyme in heme biosynthesis (Ponka, 1999). The data depicted in Figures 5A and 5B and Figure S5 show that *Por* mRNA accumulation followed a robust circadian cycle and that the peak levels of this rhythmic expression were significantly blunted in $H^{+/-}/D^{+/-}/T^{+/-}$ and $H^{-/-}/D^{-/-}/T^{-/-}$ mice. POR accumulation displayed a less pronounced circadian rhythm than *Por* mRNA but was also reduced in PAR bZip knockout mice (Figure 5C).

PAR bZip triple knockout mice have an impaired detoxification capacity

As the transcript profiling suggested an attenuated expression of many detoxification genes in PAR bZip triple knockout

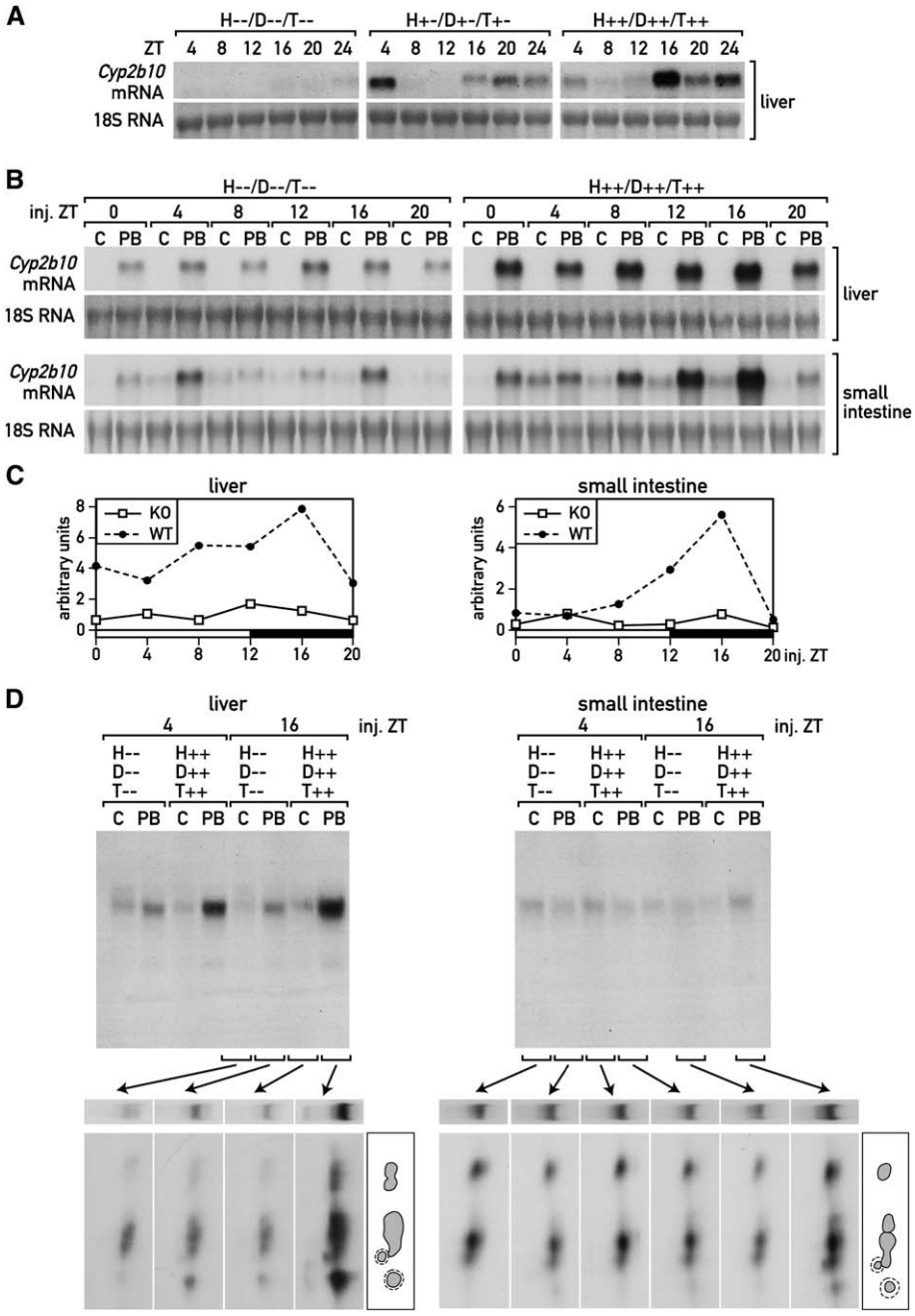

Figure 4. Control of *Cyp2b10* transcription by PAR bZip proteins

A) Temporal accumulation of *Cyp2b10* mRNA in the liver of untreated mice with the indicated genotypes.

B) *Cyp2b10* mRNA accumulation in liver (upper panels) and small intestine (lower panels) of mice with the indicated genotypes injected at the specified *Zeitgeber* times. Organs were harvested 4 hr after the saline (C) or phenobarbital (PB) (100 mg/kg, i.p.) injections. Note that the autoradiographs depicted in (**A**) and (**B**) cannot be directly compared. In (**A**), the Northern blot membrane was exposed for 2 weeks with intensifier screen, while in (**B**), the Northern blot membrane was exposed for 5 hr without intensifier screen.

C) Phosphoimager quantification of the Northern blot data displayed in (**B**). Note that phenobarbital-induced *Cyp2b10* mRNA accumulation is circadian in wild-type animals with a 2.5-fold and 8-fold amplitude in liver and small intestine, respectively. In PAR bZip triple knockout mice the induced *Cyp2b10* mRNA levels are generally lower than in wild-type mice and do not follow a circadian trend.

D) In vitro binding of the NR1 site (of the *Cyp2b10* promoter) to liver and small intestine nuclear proteins harvested before and 2 hr after phenobarbital treatment. One-dimensional and two-dimensional EMSA experiments are shown in the upper and lower panels, respectively. C: control; PB: samples obtained from phenobarbital-injected animals. The *Zeitgeber* times of injection and the genotypes of the animals are given on top of the panels. The drawings to the right of the bottom panels show a schematic representation of the spots. Note that the two signals surrounded by dotted circles are only observed after phenobarbital treatment.

mice, we wondered whether these changes in gene expression have physiological consequences. Indeed, we observed that both male and female triple knockout animals displayed an increase in liver mass (Figure 6A), which has previously been associated with xenobiotic stress. For example, a similar phenotype has been observed in mice with a liver-specific disruption of the *Por* gene (Gu et al., 2003; Henderson et al., 2003). PAR bZip knockout mice also have significantly increased plasma levels of alanine aminotransferase (F.G. and U.S., unpublished results), a diagnostic marker for liver damage (Salaspuro, 1987).

In order to investigate the sensitivity of PAR bZip-deficient mice to xenobiotic substances, we exposed wild-type and PAR bZip knockout mice to xenobiotics known to be metabolized by cytochrome P450 enzymes. First, we examined wild-type and PAR bZip triple knockout mice for the duration of sleep caused by a low dose of pentobarbital (25 mg/kg). This treatment induced a loss of the righting reflex in 90% of the wild-type mice at ZT4, but only in 50% at ZT16, and elicited an average sleeping time of 9 min and 3 min at ZT4 and ZT16, respectively (Figure 6B). All triple knockout mice lost the righting reflex irrespective of injection time and, on average, slept for 56 min and 48 min after the pentobarbital injection at ZT4 and ZT16, respectively. These results confirm the circadian regulation of drug metabolism in wild-type mice and underscore the important role of PAR bZip proteins in this process.

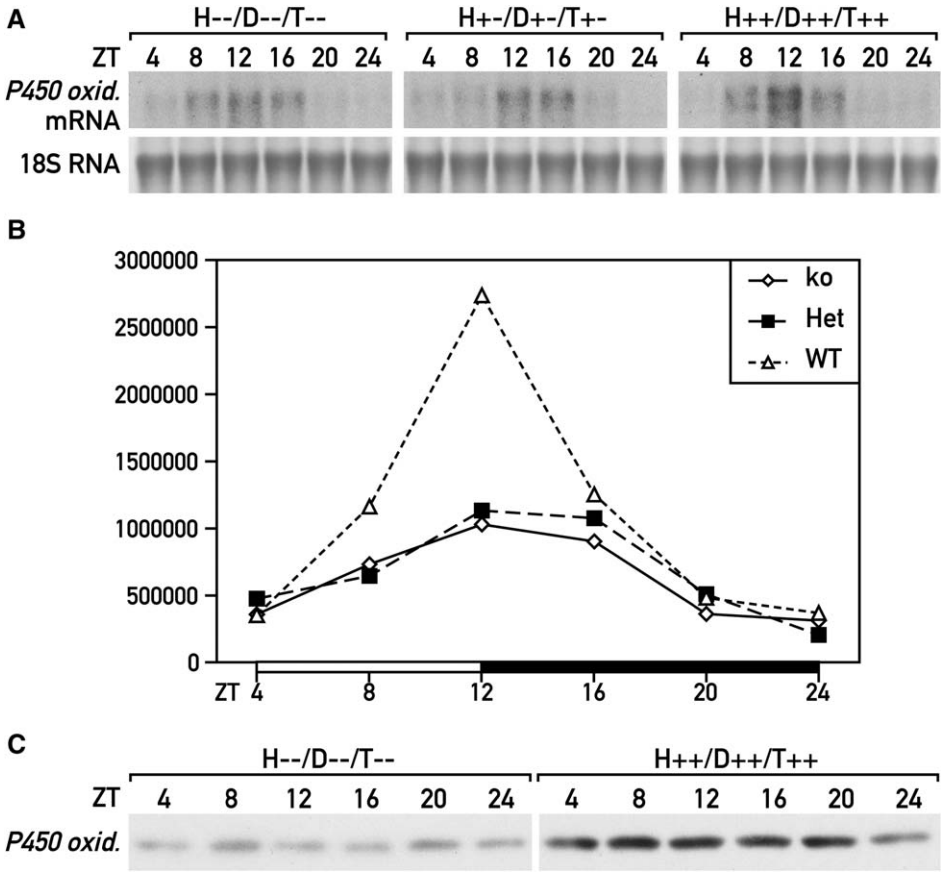

Figure 5. POR expression is downregulated in triple knockout mice

A) Temporal accumulation of *P450 oxidoreductase* (POR) mRNAs in liver, as visualized by Northern blot hybridization. Methylene blue-stained 18S rRNAs are shown as loading references. The *Zeitgeber* times (ZT) at which the animals were sacrificed are indicated on top of the figure.

B) Phosphorimager quantification of the Northern blot data displayed in (**A**).

C) Temporal POR protein accumulation in liver microsomes.

The toxicity of many anticancer drugs are known to be daytime dependent (for review see Mormont and Levi, 2003), and we wished to examine whether PAR bZip proteins are also implicated in the metabolism of such drugs. Cyclophosphamide, mitoxantrone, vincristine, and methotrexate, four chemotherapeutics whose toxicity is lowest at times when PAR bZip target gene expression is high (Gorbacheva et al., 2005; Levi et al., 1994), were injected intraperitoneally at ZT12 (see Experimental Procedures), and the toxicity was monitored by recording body mass loss and survival (Gorbacheva et al., 2005). While vincristine and methotrexate showed no significant differences in toxicity between wild-type and triple knockout mice, both mitoxantrone and cyclophosphamide were much more harmful for PAR bZip-deficient as compared to PAR bZip-proficient animals (Figures 6C and 6D).

Discussion

Many lipophilic substances, such as hormones and drugs, have been known for decades to act in a daytime-dependent manner (Mormont and Levi, 2003; Youan, 2004). Here we present data indicating that PAR bZip proteins play an important role in this process. Transcriptome profiling in liver and kidney of mice deficient for DBP, TEF, and HLF indicated that these proteins stimulated the transcription of genes encoding enzymes and regulators with important functions in the defense against xenobiotic and oxidative stress. These include genes specifying carboxylesterases, cytochrome P450 enzymes, aminolevulinic acid synthase (ALAS1), P450-oxidoreductase (POR), sulfotransferases, glutathione-S-transferases (GST), aldehyde dehydrogenases, UDP-glucuronosyltransferases, members of drug transporter families, and CAR. While some of these genes are probably direct target genes of PAR bZip transcription factors, others may be regulated indirectly through CAR. In the presence of some xenobiotic (e.g., barbiturates) and endobiotic (e.g., bilirubin) activators, CAR dissociates from its complex with chaperones and stimulates target gene expression as a heterodimer with RXR isoforms (Handschin and Meyer, 2005; Qatanani and Moore, 2005). Pregnane X Receptor (PXR) is another important sensor of xenobiotic compounds, and CAR and PXR display considerable overlap in their action (for review see Handschin and Meyer, 2005; Hartley et al., 2004; Maglich et al., 2002; Rosenfeld et al., 2003; Wei et al., 2002). However, PXR expression does not appear to be regulated by PAR bZip transcription factors in liver (Figure S5).

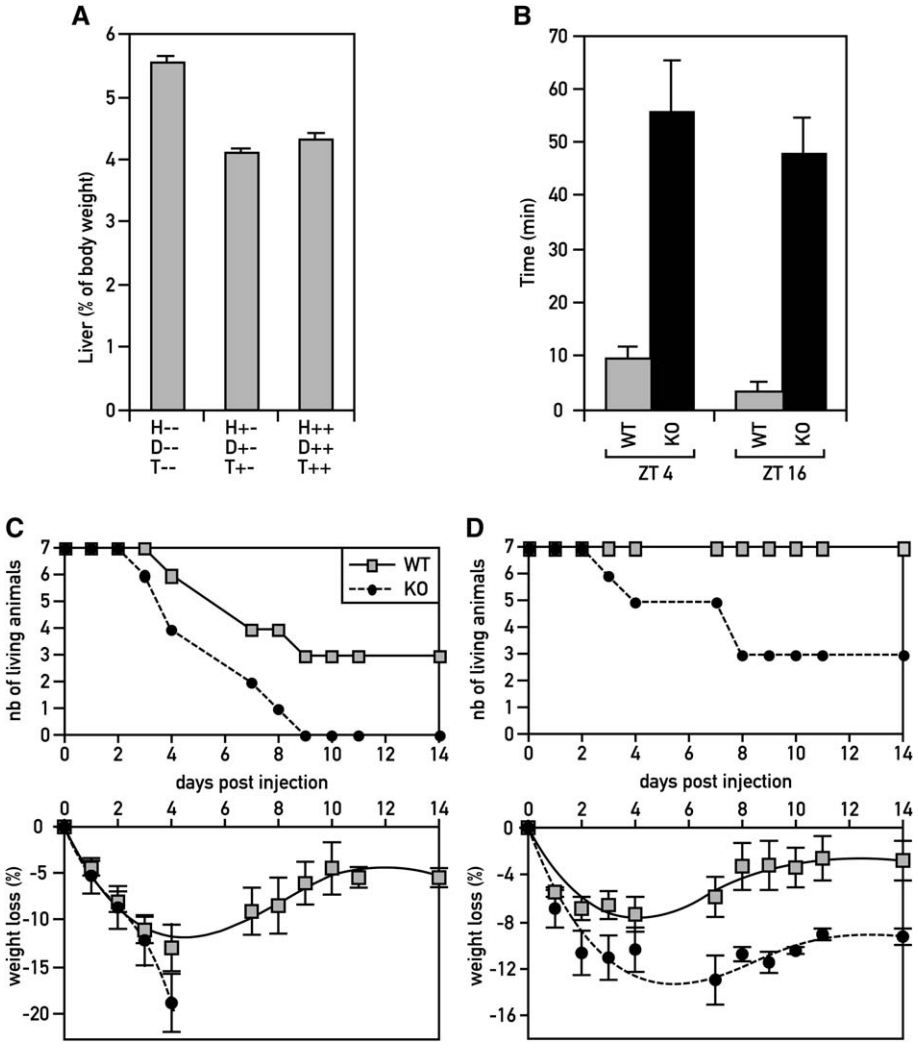

Figure 6. Manifestations of the detoxification deficiency in PAR bZip triple knockout mice

A) Increased liver mass in triple knockout mice. The body and liver mass of mice aged 3 to 4 months and belonging to the three different genotypes indicated below the panel were determined. Values represent average ratio percentages ± SEM (n = 25). Student's t tests revealed highly significant differences between triple knockout and triple heterozygous ($p \leq 1.10^{-11}$) or wild-type ($p \leq 5.10^{-9}$) mice.

B) Decreased pentobarbital clearance in triple knockout mice. Young adult mice were injected intraperitoneally with pentobarbital (25 mg/kg) at ZT4 or 16. The length of time in minutes represents the average time between the loss and subsequent recovery of the righting reflex. Values presented are means ± SEM (n = 10). Student's t test revealed a significant difference between the sleep duration of wild-type animals injected at ZT4 and ZT16 ($p \leq 0.025$), indicating a daytime-dependent difference in pentobarbital clearance. In PAR bZip knockout mice, the sleeping times were not significantly different after injection of pentobarbital at ZT4 and ZT16. However, after both times of injection, sleep duration was much longer in knockout than in wild-type animals ($p \leq 2 \times 10^{-3}$ at ZT4; $p \leq 2 \times 10^{-4}$ at ZT16).

C and D) Increased toxicity of anticancer drugs in triple knockout mice. Wild-type and triple knockout mice were injected intraperitoneally at ZT12 with mitoxantrone (10 mg/kg) (**C**) or cyclophosphamide (300 mg/kg) (**D**). The upper panel shows the mortality rate of mice after the injection, and the lower panel the average mass loss ± SEM.

Hepatocytes and epithelial villi cells of the small intestine are the only cells known to express CAR at high levels (Swales and Negishi, 2004; Wei et al., 2002). Our results suggested that phenobarbital-induced activation of CAR was circadian in both of these cell types. Interestingly, the daytime- and presumably CAR-dependent induction of *Cyp2b10* mRNA accumulation by phenobarbital displayed a higher circadian amplitude in epithelial villi cells (8-fold) as compared to hepatocytes (2.5-fold).

The induction of functionally active cytochrome P450 enzymes necessitates the simultaneous production of heme, and ALAS1 expression is indeed both circadian and inducible by activated CAR. Likewise, the production of POR, the enzyme providing electrons for all cytochrome P450-mediated monooxygenase reactions, is coordinated with that of cytochrome P450 enzymes, with regard to both daytime-dependent and inducible expression (Maglich et al., 2002; Oishi et al., 2003; Ueda et al., 2002). Importantly, PAR bZip proteins modulate the expression of both ALAS1 and POR. Lee and coworkers have recently proposed that *Alas1* transcription is regulated by the PAS helix-loop-helix protein NPAS2, a paralog of CLOCK (Kaasik and Lee, 2004). However, *Alas1* mRNA still accumulates in a circadian manner in NPAS2 mutant mice, albeit with a reduced magnitude and a delayed phase. We propose that this residual circadian expression is accounted for by PAR bZip proteins, and that the circadian expression of *Alas1* in wild-type mice is governed by the combined action of NPAS2 and PAR bZip proteins. Of note, ALAS1 is a pyridoxal phosphate (PLP)-dependent enzyme (Scholnick et al., 1972), and PLP synthesis is also controlled by PAR bZip proteins (Gachon et al., 2004a).

The various levels at which PAR bZip transcription factors might intervene in the coordination of xenobiotic detoxification are schematically depicted in Figure 7. Some genes encoding detoxification enzymes (e.g., CYP2A5, CYP2C50, CES3) may be direct PAR bZip target genes. The expression of other detoxification enzymes (e.g., CYP2B10), is mostly controlled by CAR, whose circadian transcription is governed by PAR bZip proteins. Yet other players in the xenobiotic defense (e.g., ALAS1 and POR) appear to be under the control of both CAR and PAR bZip proteins. We consider it likely that the dysregulation of detoxification pathways described in this paper contributes to the high morbidity and mortality of PAR bZip-deficient animals. Remarkably, the implication of major detoxification pathways in longevity has recently emerged from a transcriptome profiling

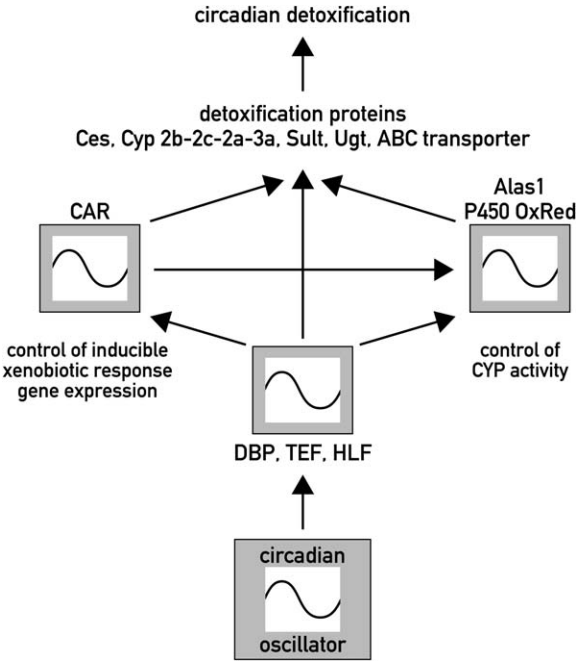

Figure 7. Model showing the different level of regulation of circadian detoxification by PAR bZip transcription factor

For explanations, see Discussion. The activation of *Dbp* transcription by the core clock components BMAL1 and CLOCK is the only interaction for which a direct mechanism has been supported by chromatin immunoprecipitation experiments and the site-directed mutagenesis of *cis*-acting elements (Ripperger and Schibler, 2006). Many of the putative PAR bZip target genes contain PARREs and display circadian transcription with a phase compatible with that of PAR bZip protein accumulation. Nevertheless, it cannot be excluded that their transcriptional regulation by DBP, HLF, and TEF involves an indirect mechanism.

study in the nematode *Caenorhabditis elegans* (McElwee et al., 2004). Signaling through the DAF-2/insulin growth factor receptor plays a particularly important role in determining the age of nematodes, and reduction of DAF-2 signaling increases life span up to 2-fold. Longevity is also extended in *dauer* larvae, a state induced by environmentally unfavorable conditions (Vanfleteren and Braeckman, 1999). A DNA microarray search for transcripts whose accumulation is upregulated in both *daf-2* mutant worms and *dauer* larvae revealed a specific enrichment for mRNAs encoding cytochrome P450 enzymes, oxidoreductases, carboxyl esterases, short-chain dehydrogenases/reductases, UDP-glucuronosyl/glucosyltransferases, sulfotransferases, and glutathione-S-transferases (McElwee et al., 2004). Accordingly, a reduced activity of such detoxification genes would be expected to promote premature aging and to reduce life span, a scenario that would be in concordance with the observations made on PAR bZip-deficient mice.

Similar to PAR bZip-deficient mice, *Clock* mutant mice are exquisitely sensitive to cyclophosphamide (Gorbacheva et al., 2005), and it is conceivable that this phenotype is a manifestation of PAR bZip downregulation in these animals (Ripperger et al., 2000; B. Kornmann and U.S., unpublished observation). Based on the pharmacokinetics of this drug measured in wild-type and mutant mice, Gorbacheva and coworkers propose that the high sensitivity of *Clock* mutant animals is caused by an increased toxicity of cyclophosphamide metabolites for the hematopoietic system. The high sensitivity of *Clock* and *PAR bZip* mutant mice to substances used as chemotherapeutics in human medicine underscores the crucial role of the circadian timekeeping system in modulating drug toxicity.

Experimental procedures

Animal care and treatment

All animal studies were conducted in accordance with the regulations of the veterinary office of the State of Geneva. Triple knockout mice with a disruption of the three PAR bZip genes *Dbp*, *Tef*, and *Hlf* have been previously described (Gachon et al., 2004a). Mice were maintained under standard animal housing conditions, with free access to food and water, and a 12 hr light/12 hr dark cycle.

Intraperitoneal phenobarbital injections (100 mg/kg) were performed at the indicated times in parallel to saline injection (control). Mice were sacrificed 2 hr and 4 hr after drug injection for the analysis of nuclear proteins and mRNA, respectively.

For the determination of pentobarbital-induced sleep time, a single intraperitoneal injection of pentobarbital (25 mg/kg) was conducted at the indicated time. The time span between loosing and regaining the righting reflex was determined.

For drug toxicity experiments, mice received a single intraperitoneal injection of mitoxantrone (10 mg/kg) or cyclophosphamide (300 mg/kg), vincristine (1 mg/kg), or methotrexate (50 mg/kg). Drug-induced toxicity was assessed by daily control of body mass loss and mortality. The loss of more than 15% of the original mass was considered the end point of the experiment. Average body mass loss values were calculated when the data from at least three mice were available.

RNA isolation and analysis

Livers and kidneys from approximately 4-month-old mice were removed within 4 min after decapitation, frozen in liquid nitrogen, and stored at −70°C until use. For the preparation of RNA from small intestine, which contains high ribonuclease levels, tissue was immediately homogenized in guanidium thiocyanate lysis buffer. The extraction of whole-cell RNA and its analysis by ribonuclease protection assays were performed as described (Schmidt and Schibler, 1995). The antisense RNA probe was transcribed from a pBluescript-KS$^+$ vector containing an RT-PCR product of mouse *Cyp2c50* mRNA (+555 to +885), *Cyp2a4* mRNA (+1533 to +1727), *Cyp2a5* mRNA (+1449 to +1691), and *Tbp* mRNA (+36 to +135). In all cases, the plasmids were linearized with a suitable restriction enzyme and the antisense RNA probes were prepared by in vitro transcription of the linearized templates with T7 or T3 RNA polymerase using [α-^{32}P].UTP.

For Northern blot experiments, 5 μg of RNA were separated in 4% formaldehyde agarose gels, blotted onto nylon membranes, and hybridized to ^{32}P-labeled single-stranded antisense DNA probes. As templates, we used pBluescript-KS$^+$ vectors containing RT-PCR products of mouse *AK3l1* mRNA (+83 to +754), *CAR* mRNA (+148 to +1119), *Alas1* mRNA (+1030 to +2090), *RGS16* mRNA (+121 to +726), *Ces3* mRNA (+969 to +1912), *Bhmt* mRNA (+65 to +1288), *Cyp2b10* mRNA (+1 to +1021), and *P450 oxidoreductase* mRNA (+210 to +1210). In all cases, the plasmids were linearized with a suitable restriction enzyme and the antisense single-stranded DNA probes were prepared by linear PCR of the linearized templates with the reverse sequencing primer and [α-^{32}P].dCTP. Hybridizations were carried out overnight at 65°C for 16 hr in Church Buffer (0.5 M Na-phosphate pH 7.0; 7% SDS and 1 mM EDTA) (Church and Gilbert, 1984). Following hybridization, the membranes were washed four times for 15 min at 65°C in 40 mM Na-phosphate pH 7.0; 1% SDS and 1 mM EDTA.

Cyp2c50 pre-mRNA levels were quantified by Taqman real-time RT-PCR. 0.5 μg of liver whole-cell RNA was reverse-transcribed using random hexamers and Superscript reverse transcriptase (Gibco, San Diego). The cDNA equivalent to 20 ng of total RNA was PCR-amplified in an ABI PRISM 7700 detection system (PE-Applied Biosystems, Foster City). The primers used were as follows: *Cyp2c50* forward: 5′-TGCCAGGCACTGGAATAGC-3−; *Cyp2c50* reverse: 5′-TTGCATTTGCCTGGAGGATT-3′; *Cyp2c50* probe: 5′-FAM-TAAGAGACAGCTATCAGGGTCCCTTCAGCA-TAMRA-3′; *Tbp* forward: 5′-TTGACCTAAAGACCATTGCACTTC-3′; *Tbp* reverse: 5′-TTCTCAT GATGACTGCAGCAAA-3′; *Tbp* probe: 5′-FAM-TGCAAGAAATGCTGAATA TAATCCCAAGCG-TAMRA-3′.

Affymetrix oligonucleotide microarray hybridization

For the first experiment, 30 wild-type mice (15 males and 15 females) and 30 triple knockout mice of approximately the same age (109 ± 16 and 113 ± 11 days, respectively) were killed at ZT15 and their livers were quickly removed, frozen on liquid nitrogen, and stored at −80ºC. RNA pools for a given genotype were assembled by mixing equal amounts of RNA from 10 animals (5 males and 5 females). Fifteen micrograms of total RNA from each pool was used to synthesize biotinylated cRNA according to the Affymetrix protocol (kits of Invitrogen for cDNA synthesis and Enzo for biotinylated cRNA synthesis). Ten micrograms of biotinylated cRNA was hybridized to mouse Affymetrix Mouse Genome 430 2.0 array.

For the second experiment, 18 triple-heterozygous mice (9 males and 9 females) and 18 triple knockout mice of approximately the same age (100 ± 5 and 107 ± 9 days, respectively) were killed at ZT12, and their livers and kidneys were quickly removed, frozen in liquid nitrogen, and stored at −80ºC. RNA pools for a given genotype were assembled by mixing equal amounts of RNA from six animals (three males and three females). Five micrograms of total RNA from each pool were used to synthesize biotinylated cRNA according to the Affymetrix protocol (Affymetrix kit). Ten micrograms of biotinylated cRNA were hybridized to mouse Affymetrix Mouse Genome 430 2.0 array according to standard procedures. To identify differentially expressed transcripts, pairwise comparisons were carried out using the Affymetrix GCOS 1.2 software. Each of the three experimental samples was compared to each of the three reference samples, resulting in nine pairwise comparisons. This approach, which is based on the Mann-Whitney pairwise comparison test, allows the ranking of results by concordance, as well as the calculation of significance (p value) for each identified change in gene expression (Hubbell et al., 2002; Liu et al., 2002). Genes for which the concordance in the pairwise comparisons exceeded a threshold were considered to be statistically significant. This conservative analytical approach was used to limit the number of false-positives. A 66% (six of nine comparisons) cutoff in the consistency of the changes was then applied to identify potential dimorphically regulated genes/ESTs. In addition, we only selected genes if they had an average change of at least 1.2-fold and if the transcript was scored as present in at least two out of three samples of the genotype yielding the higher expression values (see Tables S1, S2, and S3).

Nuclear protein extraction and analysis

Liver and small intestine nuclear proteins were prepared by using the NaCl-Urea-NP40 (NUN) procedure (Lavery and Schibler, 1993). For electromobility shift assays (EMSA) with PAR bZip binding sites, the radiolabeled probes were prepared by annealing two oligonucleotides encompassing the PAR bZip binding site and by filling in the 5′ overhang with [α-^{32}P].dCTP and Klenow DNA polymerase. The sequences of these oligonucleotides were 5′-AGCTTAGATTACATAAC-3′ and 5′-CAGCTCAGTTATGTAATCTAAGCT-3′ for *Ces3* and 5′-CTCCCGGCTTACGTAAG-3′ and 5′-GCTGCTTCTTACGTAAGCCGGGAG-3′ for *AK3l1*. Twenty micrograms of liver nuclear extract were incubated with 100 fmol of the double-stranded oligonucleotide in a 20 μl reaction containing 25 mM HEPES (pH 7.6), 60 mM KCl, 5 mM $MgCl_2$, 0.1 mM EDTA, 7.5% glycerol, 1 mM DTT, 1 μg/μl salmon sperm DNA. After an incubation of 10 min at room temperature, 2 μl of a 15% Ficoll solution were added, and the protein-DNA complexes were separated on a 5% polyacrylamide gel in 0.25 × TBE.

The radiolabeled azido-dUTP-substituted double-stranded oligonucleotide probes were prepared by annealing two oligonucleotides (encompassing the NR1 site located within the *Cyp2b10* promoter) and by filling in the 5′ overhang with azido-dUTP, [α-^{32}P].dCTP and Klenow DNA polymerase. The sequences of these oligonucleotides were 5′-AGAATCTG-3′ and 5′-CTGTGCCAAGGTCAGGAAAGTACAGATTCT-3′. Binding reactions were as described above, except that 50 fmol of the double-stranded oligonucleotide probe were used and that 0.25 nmol of an unlabeled double-stranded oligonucleotide corresponding to a mutated NR1 site (sequence 5′-AGAATC gaTgtTaaCCgtACtcgGGCACAG-3′, mutated positions in lower case letters) was added to increase the specificity of EMSA. After an incubation period of 10 min at room temperature, 5 μl of a 15% Ficoll solution was added, and the protein-DNA complexes were separated on a 5% polyacrylamide gel in 0.25 × TBE.

For the two-dimensional EMSA (Ossipow et al., 1993), the reaction was assembled as described above with 50 μg of protein in a volume of 40 μl. The complexes were resolved on a 5% polyacrylamide gel in 0.25 × TBE and then UV-crosslinked in the gel for 15 min at 254 nm. The polyacrylamide strip containing the crosslinked material was placed horizontally on an SDS/8% polyacrylamide gel. Supershift EMSA experiments with the CAR recognition sequence included 10 μg of a CAR antibody (kindly provided by Masahiko Negishi, NIH) during a 10 min preincubation incubation without DNA probes (Figure S9).

Western blot analysis of microsomal proteins

Microsomal proteins were prepared as described (Giger and Meyer, 1981), with small modifications. Briefly, snap-frozen liver tissue was homogenized in 0.2 M Na-phosphate pH 7.0, and the homogenate was cleared by a 20 min centrifugation at 9000 g. Microsomal fractions were recovered from the supernatant by a 1 hr centrifugation at 105000 g. After resuspension of the pellet in NUN buffer (Lavery and Schibler, 1993) (see above), 10 μg of microsomal proteins was resolved on an SDS/8% polyacrylamide gel and transferred to a nitrocellulose membrane for the Western blot analysis. Rabbit P450 oxidoreductase polyclonal antibody was kindly provided by Urs Meyer, Basel.

Affymetrix microarray hybridization data

All Affymetrix microarray hybridization data are available at MIAMExpress, accession number E-MEXP-565.

Supplemental data

Supplemental data include nine figures and can be found with this article online at http://www.cellmetabolism.org/cgi/content/full/4/1/25/DC1/.

Acknowledgments

We are most grateful to Mylène Docquier and Didier Chollet (Genomics Platform of the NCCR program Frontiers in Genetics) for their invaluable help in the Affymetrix transcriptome profiling studies and to Pascal Gos for his assistance in genotyping the various mutant mice. Urs Meyer (Biocenter, University of Basel) generously provided POR antibodies and gave us advice on the preparation of microsomes. We also would like to thank Masahiko Negishi (NIH, Research Triangle Park, NC) for the CAR antibody, Gerhard Wanner (Department of Applied Mathematics, University of Geneva) for his help in mathematical modeling of circadian mRNA accumulation, and Nicolas Roggli for his expert preparation of the artwork. The critical comments on our manuscript by Urs Meyer (Biocenter, University of Basel), Catherine Legraverend (Institut de Génomique Fonctionelle, Montpellier), and by our laboratory colleagues Charna Dibner, Hans Reinke, and David Gatfield were greatly appreciated.

This research was supported by the Swiss National Science Foundation (through an individual research grant to U.S. and the NCCR program *Frontiers in Genetics*), the State of Geneva, the *Louis Jeantet Foundation of Medicine*, and the *Bonizzi-Theler Stiftung*.

Received: January 13, 2006
Revised: March 21, 2006
Accepted: April 27, 2006
Published: July 4, 2006

References

Anzenbacher, P., and Anzenbacherova, E. (2001). Cytochromes P450 and metabolism of xenobiotics. Cell. Mol. Life Sci. *58*, 737–747.

Church, G.M., and Gilbert, W. (1984). Genomic sequencing. Proc. Natl. Acad. Sci. USA *81*, 1991–1995.

Falvey, E., Fleury-Olela, F., and Schibler, U. (1995). The rat hepatic leukemia factor (HLF) gene encodes two transcriptional activators with distinct circadian rhythms, tissue distributions and target preferences. EMBO J. *14*, 4307–4317.

Falvey, E., Marcacci, L., and Schibler, U. (1996). DNA-binding specificity of PAR and C/EBP leucine zipper proteins: a single amino acid substitution in

the C/EBP DNA-binding domain confers PAR-like specificity to C/EBP. Biol. Chem. *377*, 797–809.

Fonjallaz, P., Ossipow, V., Wanner, G., and Schibler, U. (1996). The two PAR leucine zipper proteins, TEF and DBP, display similar circadian and tissue-specific expression, but have different target promoter preferences. EMBO J. *15*, 351–362.

Franken, P., Lopez-Molina, L., Marcacci, L., Schibler, U., and Tafti, M. (2000). The transcription factor DBP affects circadian sleep consolidation and rhythmic EEG activity. J. Neurosci. *20*, 617–625.

Gachon, F., Fonjallaz, P., Damiola, F., Gos, P., Kodama, T., Zakany, J., Duboule, D., Petit, B., Tafti, M., and Schibler, U. (2004a). The loss of circadian PAR bZip transcription factors results in epilepsy. Genes Dev. *18*, 1397–1412.

Gachon, F., Nagoshi, E., Brown, S.A., Ripperger, J., and Schibler, U. (2004b). The mammalian circadian timing system: from gene expression to physiology. Chromosoma *113*, 103–112.

Giger, U., and Meyer, U. (1981). Induction of delta-aminolevulinate synthase and cytochrome P-450 hemoproteins in hepatocyte culture. Effect of glucose and hormones. J. Biol. Chem. *256*, 11182–11190.

Gorbacheva, V.Y., Kondratov, R.V., Zhang, R., Cherukuri, S., Gudkov, A.V., Takahashi, J.S., and Antoch, M.P. (2005). Circadian sensitivity to the chemotherapeutic agent cyclophosphamide depends on the functional status of the CLOCK/BMAL1 transactivation complex. Proc. Natl. Acad. Sci. USA *102*, 3407–3412.

Gu, J., Weng, Y., Zhang, Q.Y., Cui, H., Behr, M., Wu, L., Yang, W., Zhang, L., and Ding, X. (2003). Liver-specific deletion of the NADPH-cytochrome P450 reductase gene: impact on plasma cholesterol homeostasis and the function and regulation of microsomal cytochrome P450 and heme oxygenase. J. Biol. Chem. *278*, 25895–25901.

Gutierrez, A., Grunau, A., Paine, M., Munro, A.W., Wolf, C.R., Roberts, G.C.K., and Scrutton, N.S. (2003). Electron transfer in human cytochrome P450 reductase. Biochem. Soc. Trans. *31*, 497–501.

Handschin, C., and Meyer, U.A. (2005). Regulatory network of lipid-sensing nuclear receptors: roles for CAR, PXR, LXR, and FXR. Arch. Biochem. Biophys. *433*, 387–396.

Hartley, D.P., Dai, X., He, Y.D., Carlini, E.J., Wang, B., Huskey, S.E., Ulrich, R.G., Rushmore, T.H., Evers, R., and Evans, D.C. (2004). Activators of the rat pregnane X receptor differentially modulate hepatic and intestinal gene expression. Mol. Pharmacol. *65*, 1159–1171.

Henderson, C.J., Otto, D.M., Carrie, D., Magnuson, M.A., McLaren, A.W., Rosewell, I., and Wolf, C.R. (2003). Inactivation of the hepatic cytochrome P450 system by conditional deletion of hepatic cytochrome P450 reductase. J. Biol. Chem. *278*, 13480–13486.

Honkakoski, P., Zelko, I., Sueyoshi, T., and Negishi, M. (1998). The nuclear orphan receptor CAR-retinoid X receptor heterodimer activates the phenobarbital-responsive enhancer module of the CYP2B gene. Mol. Cell. Biol. *18*, 5652–5658.

Hubbell, E., Liu, W.-M., and Mei, R. (2002). Robust estimators for expression analysis. Bioinformatics *18*, 1585–1592.

Kaasik, K., and Lee, C.C. (2004). Reciprocal regulation of haem biosynthesis and the circadian clock in mammals. Nature *430*, 467–471.

Lavery, D.J., and Schibler, U. (1993). Circadian transcription of the cholesterol 7 alpha hydroxylase gene may involve the liver-enriched bZIP protein DBP. Genes Dev. *7*, 1871–1884.

Levi, F., Tampellini, M., Metzger, G., Bizi, E., Lemaigre, G., and Hallek, M. (1994). Circadian changes in mitoxantrone toxicity in mice: relationship with plasma pharmacokinetics. Int. J. Cancer *59*, 543–547.

Liu, W.-m., Mei, R., Di, X., Ryder, T.B., Hubbell, E., Dee, S., Webster, T.A., Harrington, C.A., Ho, M.-h., Baid, J., and Smeekens, S.P. (2002). Analysis of high density expression microarrays with signed-rank call algorithms. Bioinformatics *18*, 1593–1599.

Lopez-Molina, L., Conquet, F., Dubois-Dauphin, M., and Schibler, U. (1997). The DBP gene is expressed according to a circadian rhythm in the suprachiasmatic nucleus and influences circadian behavior. EMBO J. *16*, 6762–6771.

Maglich, J.M., Stoltz, C.M., Goodwin, B., Hawkins-Brown, D., Moore, J.T., and Kliewer, S.A. (2002). Nuclear pregnane X receptor and constitutive androstane receptor regulate overlapping but distinct sets of genes involved in xenobiotic detoxification. Mol. Pharmacol. *62*, 638–646.

Maglich, J.M., Watson, J., McMillen, P.J., Goodwin, B., Willson, T.M., and Moore, J.T. (2004). The nuclear receptor CAR is a regulator of thyroid hormone metabolism during caloric restriction. J. Biol. Chem. *279*, 19832–19838.

McElwee, J.J., Schuster, E., Blanc, E., Thomas, J.H., and Gems, D. (2004). Shared transcriptional signature in Caenorhabditis elegans Dauer larvae and long-lived daf-2 mutants implicates detoxification system in longevity assurance. J. Biol. Chem. *279*, 44533–44543.

Mormont, M.-C., and Levi, F. (2003). Cancer chronotherapy: Principles, applications, and perspectives. Cancer *97*, 155–169.

Oishi, K., Miyazaki, K., Kadota, K., Kikuno, R., Nagase, T., Atsumi, G.-i., Ohkura, N., Azama, T., Mesaki, M., Yukimasa, S., et al. (2003). Genome-wide expression analysis of mouse liver reveals CLOCK-regulated circadian output genes. J. Biol. Chem. *278*, 41519–41527.

Ossipow, V., Descombes, P., and Schibler, U. (1993). CCAAT/enhancer-binding protein mRNA is translated into multiple proteins with different transcription activation potentials. Proc. Natl. Acad. Sci. USA *90*, 8219–8223.

Ponka, P. (1999). Cell biology of heme. Am. J. Med. Sci. *318*, 241–256.

Qatanani, M., and Moore, D.D. (2005). CAR, the continuously advancing receptor, in drug metabolism and disease. Curr. Drug Metab. *6*, 329–339.

Reppert, S.M., and Weaver, D.R. (2002). Coordination of circadian timing in mammals. Nature *418*, 935–941.

Ripperger, J., and Schibler, U. (2006). Rhythmic CLOCK-BMAL1 binding to multiple E-box motifs drives circadian Dbp transcription and chromatin transitions. Nat. Genet. *38*, 369–374.

Ripperger, J.A., Shearman, L.P., Reppert, S.M., and Schibler, U. (2000). CLOCK, an essential pacemaker component, controls expression of the circadian transcription factor DBP. Genes Dev. *14*, 679–689.

Rosenfeld, J.M., Vargas, R., Jr., Xie, W., and Evans, R.M. (2003). Genetic profiling defines the xenobiotic gene network controlled by the nuclear receptor pregnane X receptor. Mol. Endocrinol. *17*, 1268–1282.

Salaspuro, M. (1987). Use of enzymes for the diagnosis of alcohol-related organ damage. Enzyme *37*, 87–107.

Satoh, T., and Hosokawa, M. (1998). THE MAMMALIAN CARBOXYLESTERASES: from molecules to functions. Annu. Rev. Pharmacol. Toxicol. *38*, 257–288.

Schmidt, E.E., and Schibler, U. (1995). Cell size regulation, a mechanism that controls cellular RNA accumulation: consequences on regulation of the ubiquitous transcription factors Oct1 and NF-Y and the liver-enriched transcription factor DBP. J. Cell Biol. *128*, 467–483.

Scholnick, P.L., Hammaker, L.E., and Marver, H.S. (1972). Soluble-aminolevulinic acid synthetase of rat liver. II. Studies related to the mechanism of enzyme action and hemin inhibition. J. Biol. Chem. *247*, 4132–4137.

Staudinger, J.L., Madan, A., Carol, K.M., and Parkinson, A. (2003). Regulation of drug transporter gene expression by nuclear receptors. Drug Metab. Dispos. *31*, 523–527.

Swales, K., and Negishi, M. (2004). CAR, driving into the future. Mol. Endocrinol. *18*, 1589–1598.

Ueda, A., Hamadeh, H.K., Webb, H.K., Yamamoto, Y., Sueyoshi, T., Afshari, C.A., Lehmann, J.M., and Negishi, M. (2002). Diverse roles of the nuclear

orphan receptor CAR in regulating hepatic genes in response to phenobarbital. Mol. Pharmacol. *61*, 1–6.

Vanfleteren, J.R., and Braeckman, B.P. (1999). Mechanisms of life span determination in Caenorhabditis elegans. Neurobiol. Aging *20*, 487–502.

Wang, H., Zhao, Y., Bradbury, J.A., Graves, J.P., Foley, J., Blaisdell, J.A., Goldstein, J.A., and Zeldin, D.C. (2004). Cloning, expression, and characterization of three new mouse cytochrome P450 enzymes and partial characterization of their fatty acid oxidation activities. Mol. Pharmacol. *65*, 1148–1158.

Wei, P., Zhang, J., Dowhan, D.H., Han, Y., and Moore, D.D. (2002). Specific and overlapping functions of the nuclear hormone receptors CAR and PXR in xenobiotic response. Pharmacogenomics J. *2*, 117–126.

Youan, B.-B.C. (2004). Chronopharmaceutics: gimmick or clinically relevant approach to drug delivery? J. Control. Release *98*, 337–353.